Load Characteristics of Engine Main Bearing : Comparison Between Theory and Experiment

Cho, Myung-Rae*, Oh, Dae-Yoon, Ryu, Seung-Hyuk
Power Train R&D Center, Hyundai Motor Co., Kyunggi-do 445-706, Korea
Han, Dong-Chul
School of Aerospace and Mechanical Engineering, Seoul National University, Seoul 151-742, Korea

The load characteristics of engine main bearing are very important in the design of crankshaft and engine block. The stiffness of crankshaft and block, or the optimal dimension of the bearing can be determined according to the load level. This paper presents the load characteristics of engine main bearing. Two components of the main bearing load are measured during engine firing and motoring. The vertical and horizontal load components are measured by using the dynamic load cell mounted in each main bearing cap bolt. The measured main bearing loads are compared with calculated results by using the statically determinate method. The theoretical results, provided in this study, agreed well with the experimental results. The presented results are very useful for achieving optimal design of engine.

Key Words : Load, Main Bearing, Crankshaft, Statically Determinate Method, Bearing Cap, Moving System

Nomenclature

A : Phase angle of rotating mass
F : Force
L : Length
M : Mass
R : Rotating radius
θ : Crank angle
ω : Angular velocity

1. Introduction

As the main source of vibration and noise in engine, the crankshaft plays a very important role in engine performance, and influences on the reliability and durability of the engine. In recent years, the tendency of engine design has become small size and low weight, but the power required in engine has been steadily increasing. Hence, the operating conditions of crankshaft have become more and more severe.

The loads on the crankshaft provide very important information to analyze the oil film thickness and behavior of the crankshaft. Also, they can be used as design criterion of crankshaft, bearing and engine block, as well as boundary conditions in FEM model.

Regarding the crankshaft load, the loads on the crank pin can be simply obtained by using the cylinder pressure and the inertia force of the piston and the connecting-rod. However, it is very difficult to obtain the loads on the crank journal by analysis, because crankshaft is a statically indeterminate system supported by multiple bearings. Also, the experiment is not easy due to the constraint of space and the difficulty of mounting the sensor.

The statically determinate method (Cho, et al., 2000) is commonly used to calculate the main bearing load. In this method, all the bearings are treated independently of each other. The other

* Corresponding Author.
E-mail : formell@hyundai-motor.com
TEL : +82-31-369-4517; **FAX** : +82-31-369-4503
Power Train R&D Center, Hyundai Motor Co., Kyunggi-do 445-706, Korea. (Manuscript **Received** November 26, 2001; **Revised** May 16, 2002)

method is that a crankshaft is treated as a flexible shaft supported by a spring and a damper, or a plain journal bearing (Gross, and Husmann, 1966; Eglof, 1970; Tinaut, et al., 2000). The finite element method is also used for more accurate analysis (Mourelatos, 1995; Prakash, et al., 1998).

The loads on the main bearings can be generally understood to measure the tensile or compressive strain of the bolt in the main bearing cap. However, it is very difficult to attach the strain gage to the engine block, and calibrate the signal. In recent years, the method to measure the vertical load by using the ring type load cell was introduced (Ishihama, et al., 1981). In this method, it is impossible to measure the horizontal load. Therefore, Tinaut, et al. (2000) measured the vertical load, and then they indirectly derived the horizontal load from the vertical component by using the multilineal regression method. However, there are some differences between the theory and the experiment, and it is impossible to know the horizontal load, if the load cell cannot detect the negative force.

In this study, vertical and horizontal load components are simultaneously measured by using two different ring type load cells. The experimental results are compared with the theoretical results by using the statically determinate method. The theoretical results agreed well with experimental results.

The usage of statically determinate method is very helpful for saving the computational time and cost to verify the performance of crankshaft and main bearing in the early stage of design.

2. Model of Crankshaft System

Figure 1 shows the schematic diagram of the crankshaft system used in this study. The crankshaft has eight balance weights, and is supported by five main bearings.

In this study, the loads on the main bearings are calculated by using the statically determinate method. In the case of in-line 4 engine, the crankshaft is treated as four independent systems

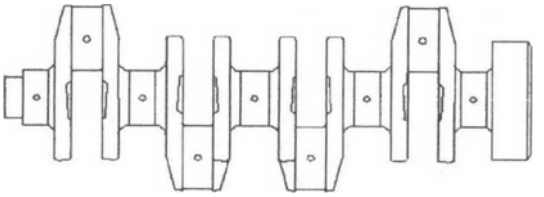

Fig. 1 Schematic diagram of 8-balance crankshaft

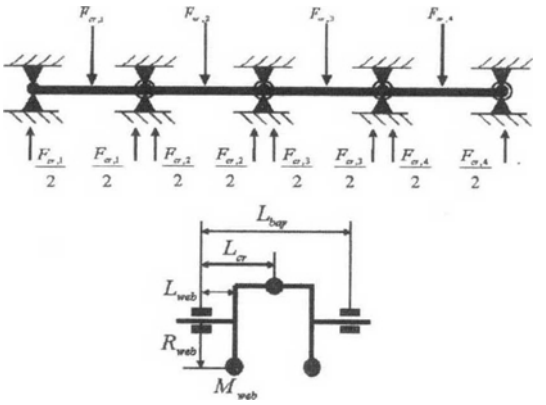

Fig. 2 Statistically determinate model of in-line 4 crankshaft system

pin-jointed at each main bearing (see Fig. 2). In this test engine, the crankshaft is composed of four bays, and a bay consists of three webs. It is also assumed that the pressure of each cylinder has only phase difference and the crankshaft is symmetric with respect to the main 3 bearing. Therefore, the load of each bearing can be obtained by analysis of half side of the crankshaft only.

From the above model, the force equilibrium of No. 1 main bearing is defined as follows:

$$F_{mx,1}-\frac{F_{crx,1}(L_{bay,1}-L_{cr,1})}{L_{bay,1}}-\frac{F_{crx,2}(L_{bay,1}-L_{cr,2})}{L_{bay,1}}+\sum_{im=1}^{nn}M_{web,im}R_{web,im}\omega_j^2\sin(A_{web,im}+\theta)\frac{[L_{bay,1}-L_{web,im}]}{L_{bay,1}}=0 \quad (1)$$

$$F_{my,1}-\frac{F_{cry,1}(L_{bay,1}-L_{cr,1})}{L_{bay,1}}-\frac{F_{cry,2}(L_{bay,1}-L_{cr,2})}{L_{bay,1}}+\sum_{im=1}^{nn}M_{web,im}R_{web,im}\omega_j^2\cos(A_{web,im}+\theta)\frac{[L_{bay,1}-L_{web,im}]}{L_{bay,1}}=0 \quad (2)$$

From the 2nd to the nn-1th bearings, the force equilibrium can be expressed as the following form

$$F_{my,2}-\frac{F_{cry,1}(L_{bay,1}-L_{cr,1})}{L_{bay,2}}-\frac{F_{cry,2}(L_{bay,2}-L_{cr,2})}{L_{bay,2}}+\sum_{im=1}^{nn}M_{web,im}R_{web,im}\omega_j^2\cos(A_{web,im}+\theta)\frac{[L_{bay,2}-L_{web,im}]}{L_{bay,2}}+\sum_{im=1}^{nn}M_{web,im}R_{web,im}\omega_j^2\cos(A_{web,im}+\theta)\frac{L_{web,im}}{L_{bay,1}}=0 \quad (3)$$

$$F_{mx,2}-\frac{F_{crx,1}(L_{bay,2}-L_{cr,1})}{L_{bay,2}}-\frac{F_{crx,2}(L_{bay,2}-L_{cr,2})}{L_{bay,2}}+\sum_{im=1}^{nn}M_{web,im}R_{web,im}\omega_j^2\sin(A_{web,im}+\theta)\frac{[L_{bay,2}-L_{web,im}]}{L_{bay,2}}+\sum_{im=1}^{nn}M_{web,im}R_{web,im}\omega_j^2\sin(A_{web,im}+\theta)\frac{L_{web,im}}{L_{bay,1}}=0 \quad (4)$$

where 'nn' means the third main bearing in the case of L-4 engine.

The force equilibrium of nnth bearing can be written as

$$F_{mx,nn}-\frac{F_{crx,1}(L_{bay,nn}-L_{cr,1})}{L_{bay,nn}}-\frac{F_{crx,2}(L_{bay,nn}-L_{cr,2})}{L_{bay,nn}}+\sum_{im=1}^{nn}M_{web,im}R_{web,im}\omega_j^2\sin(A_{web,im}+\theta)\frac{L_{web,im}}{L_{bay,im}}=0 \quad (5)$$

$$F_{my,nn}-\frac{F_{cry,1}(L_{bay,nn}-L_{cr,1})}{L_{bay,nn}}-\frac{F_{crx,2}(L_{bay,nn}-L_{cr,2})}{L_{bay,nn}}+\sum_{im=1}^{nn}M_{web,im}R_{web,im}\omega_j^2\cos(A_{web,im}+\theta)\frac{L_{web,im}}{L_{bay,im}}=0 \quad (6)$$

In Eqs. (1)~(6), the loads acting on the crank pin can be calculated from the cylinder pressure and the translating and rotating inertia forces of the piston, connecting-rod and the crank pin.

3. Experiment

In this study, the main bearing loads are measured by using the ring type quartz dynamic load cell. The compressive and shear load cells are simultaneously mounted in the bolts of the main bearing cap as can be seen in Fig. 3. The load cells are pre-loaded by using the assembling torque of the cap bolt of the main bearing. The vertical load is measured at No. 1-4 main bearings, and the horizontal load is only measured at No. 3 main bearing.

In order to know the conversion coefficient between the actual force and the output voltage of load cell, a dummy shaft was inserted in the crank journal hole and loaded with different weights

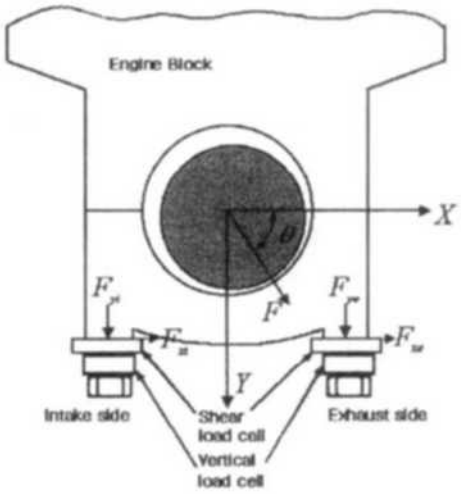

Fig. 3 Schematic diagram of load cell mounting

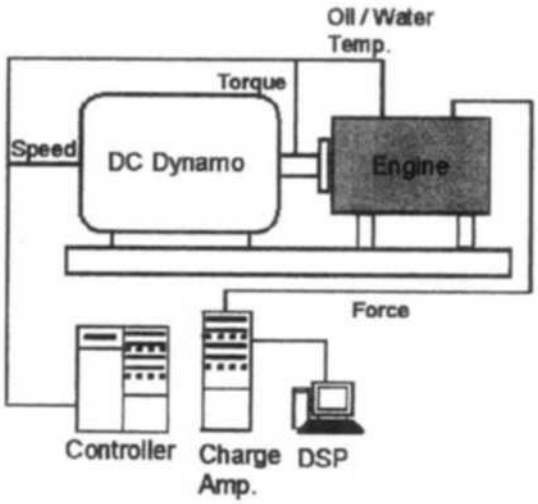

Fig. 4 Schematic diagram of engine test system

and at various angles. By adding or extracting the output signal of each load cell, the actual force can be obtamed.

Figure 4 shows the schematic diagram of the engine test rig and the data acquisition system. The experiment under the firing and motoring conditions was performed using the 110kW DC dynamometer. A 1.6L-DOHC engine was used for the test. During the test, the temperature of the cooling water was kept at 90℃ by using the water cooler. The output signal from the load cell was amplified by using the charge amplifier, and then saved in DSP system. The cyclic variation of the

Table 1 Specification of test engine

Engine type		L4/1.6D
Bore dia. (mm)		76.5
Stroke (mm)		87
Con-rod bearing	width (mm)	18
	dia. (mm)	50
Main bearing	width (mm)	16
	dia. (mm)	45
Piston Assy. mass (kg)		0.290
Crankshaft mass (kg)		13.4
Con-rod mass (kg)		0.450
Load condition		WOT (wide open throttle) Part Load Motoring

bearing load was averaged during 300 engine cycles. The specification of the test engine is described in Table 1.

4. Results and Discussion

Figure 5 shows the comparative results between theory and experiment at each bearing under the full load condition at 1500 rpm. The actual cylinder pressure is measured to use in load calculation. The crank angle of 0 degree in the cycle indicates the cylinder 1 firing TDC position

The main 1 bearing is mainly influenced by cylinder 1 (0 degree). The measured load is smaller than the calculated results. This is because the left end side of the crankshaft is supported by the timing belt rather than by bearing cap 1.

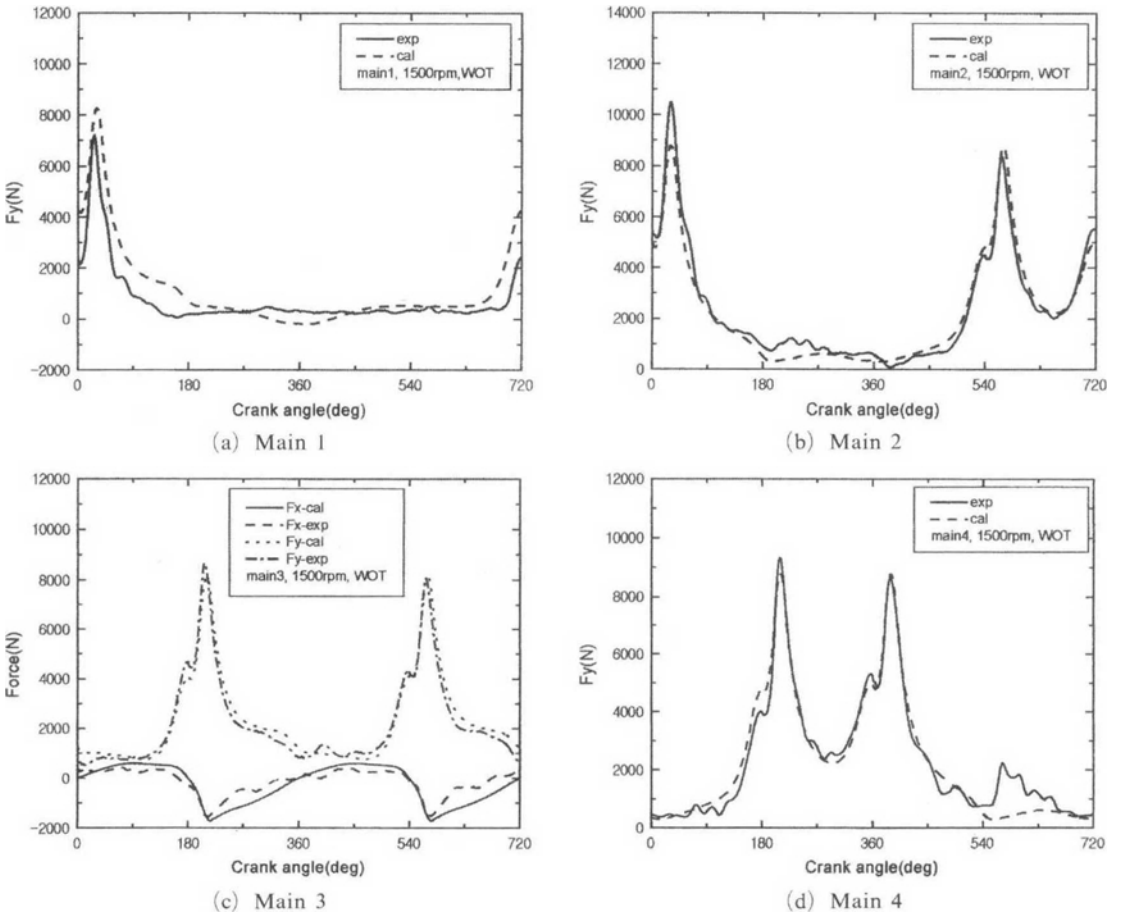

Fig. 5 The experimental and calculated bearing load in each main bearing

The main 2 bearing is influenced by cylinders 1 and 2 (540 degree), simultaneously. The effect of cylinder 1 is relatively larger than cylinder 2. This is because of the deviation of the cylinder pressure between each cylinder and deformation of crankshaft.

The main 3 bearing is at the symmetric position of the crankshaft and it is influenced by the combustion pressure of all cylinders. But the effects of cylinders 2 (540 degree) and 3 (180 degree) are relatively greater than cylinders 1 and 4 (360 degree). The cyclic variation of the horizontal force is caused by the inertia force of the rotating mass. The magnitude of the horizontal force should increase as the engine speed increases.

The main 4 bearing is affected by cylinders 3 and 4, and has a phase difference with respect to main 2 bearing.

As can be seen in Fig. 5, the maximum load of main 2 is the greatest of all bearings and the magnitude of actual force is different the according to the bearing position. As mentioned above, this is because of the pressure deviation between the cylinders, deformation of the crankshaft, and the effect of timing belt and flywheel, which are not considered in this study.

The effects of engine speed on the main 3 bearing loads are shown in Fig. 6. At high engine speed, the negative vertical force is not detected from the load cell, but the measured results agree well with calculation. At low engine speed, the cylinder pressure is the main source of bearing force. As engine speed increases, the effect of inertia force increases and the explosive force term decreases. The effect of inertia force is dominant at high engine speed in main 3 bearing.

Figure 7 shows the effect of engine speed in the main 1 and 2 bearings. The maximum force significantly increases as the engine speed increases due to increment of the cylinder pressure. The negative force is not detected in main 1 bearing. The variation of inertia force is relatively small in main 2 bearing.

Figure 8 shows the comparative results between motoring and firing conditions. As can be seen in Fig. 8, there are some differences in the absolute magnitude and position of the maximum load. This is caused by the difference in the combustion

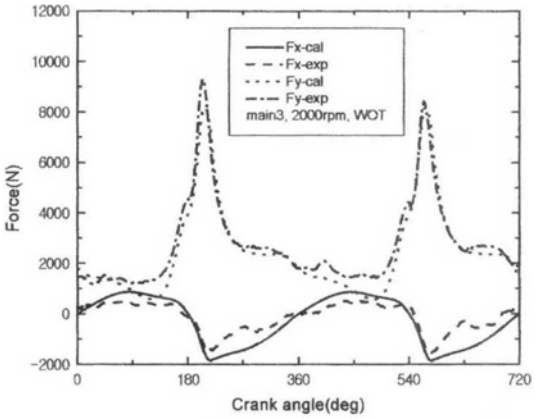

(a) 2000 rpm

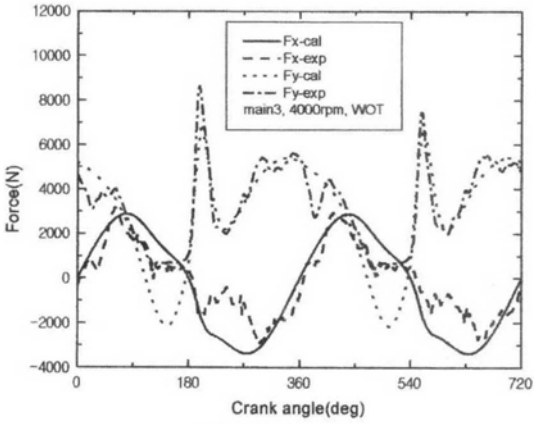

(b) 4000 rpm

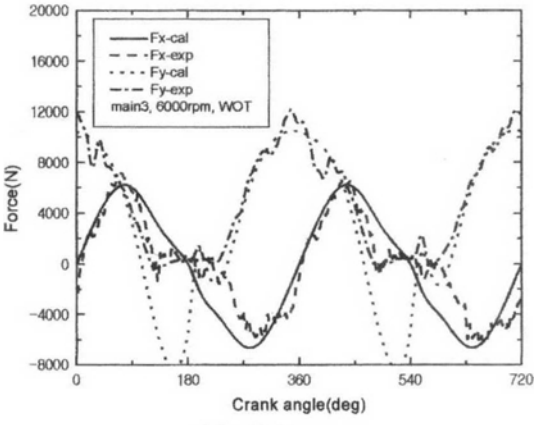

(c) 6000 rpm

Fig. 6 The effect of engine speed on the bearing load in the main 3 bearing

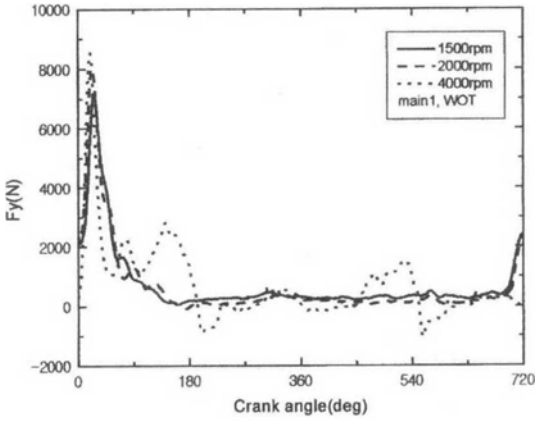

(a) Main 1

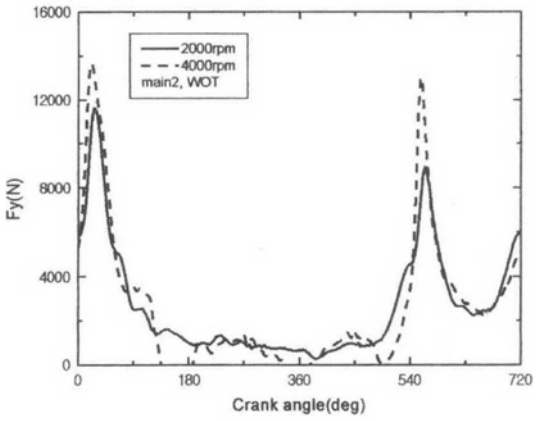

(b) Main 2

Fig. 7 The effect of engine speed on the bearing force in the main 1 and 2 bearing

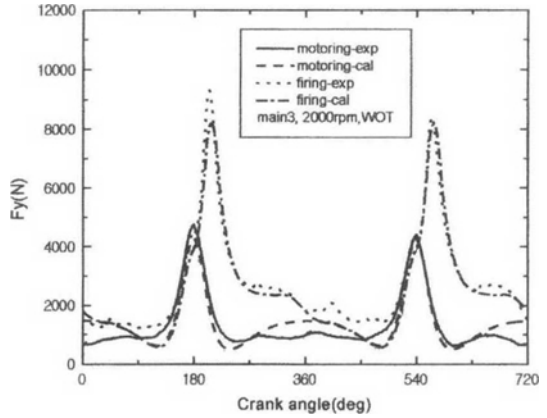

Fig. 8 The effect of engine load on the bearing reaction force in the main 3 bearing

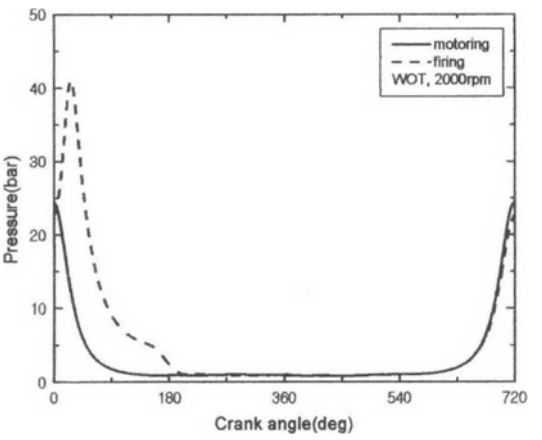

Fig. 9 Cylinder pressure variation according to the load condition

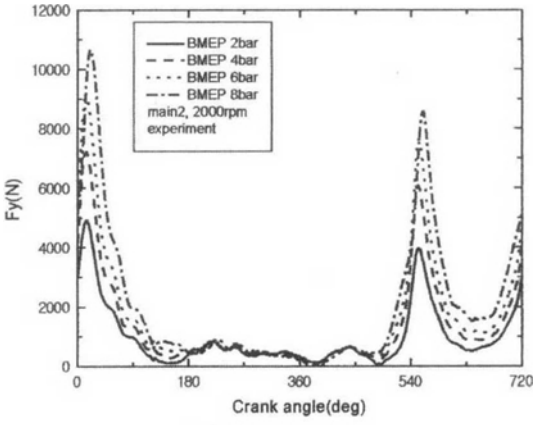

(a) Experiment

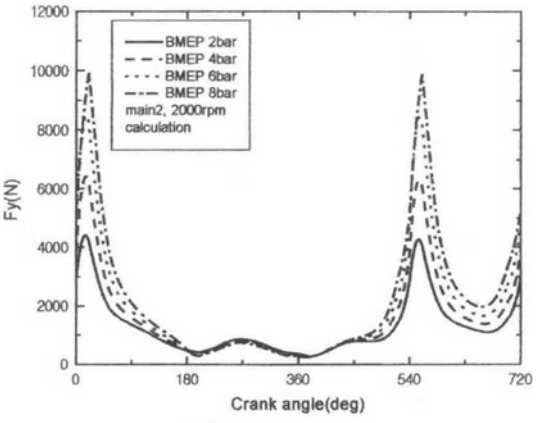

(b) Calculation

Fig. 10 The effect of load on the bearing reaction force in the main 2 bearing

process according to the operating condition and can be confirmed in Fig. 9.

Figure 10 shows the effect of engine load on the bearing reaction force. The cylinder pressure increases with increasing BMEP (break mean effective pressure). As the engine load increases, the maximum force increases due to increasing cylinder pressure. However, the inertia term is not influenced by the load change.

5. Conclusion

To investigate the load characteristics on the main bearings, the vertical and horizontal load components were measured in the main bearing caps by using the ring type load cells. Also, the main bearing loads were analyzed by using the statically determinate method, and then compared with the experimental results. The measured maximum load was generally greater than the calculated results except main 1 bearing, and the load cell could not detect negative vertical forces in main 1 and 3 bearings. However, the theoretical results, provided in this study, agree well with the experimental results.

The presented results in this study will be helpful to understand the characteristics of crankshaft load and behavior.

References

Cho, M. R., Shin, H. J. and Han, D. C., 2000, "A Study on the Circumferential Groove Effects on the Minimum Oil Film Thickness in Engine Bearings," *KSME International Journal*, Vol. 14, No. 7, pp. 737~743.

Eglof von Schnurbein, 1970, "A New Method of Calculating Plain Bearings of Statically Indeterminate Crankshafts," SAE paper 700716.

Gross, W. and Hussmann, A. W., 1966, "Forces in the Main Bearings of Multicylinder Engines," SAE paper 660756.

Ishihama, M., Hayashi, Y. and Kubozuka, T., 1981, "An Analysis of the Movement of the Crankshaft Journal During Engine Firing," SAE paper 810772.

Mourelatos, Z. P., 1995, "An Analytical Investigation of the Crankshaft Flywheel Bending Vibrations for a V6 Engine," SAE paper 951276.

Prakash, V., Aprameyan, K. and Shrinivasa, U., 1998, "An FEM Based Approach to Crankshaft Dynamics and Life Estimation," SAE paper 980565

Tinaut, F. V., Melgar, A., Gimenez, B., Fernandez, L. and Huidobro, H., 2000, "A Method to Determine the Two Components of the Crankshaft Load on a Bearing Cap in Firing Engines," SAE paper 2000-01-1340.